JARST Journal of Applied Research on Science and Technology
Rajamangala University of Technology Thanyaburi

Build-up Factors and Fast Neutron Properties of Some Plastic and Polymer for Shielding Materials: A Simulation

Sunantasak Ravangvong[1*], Punsak Glumglomchit[2], Thatchapol Hudsathapun[2], Narawich Mitdee[2], Teerawatch Ngodngam[2], Kittisak Sriwongsa[3,4] and Chumphon Khobkham[5]

[1]Division of Science and Technology, Faculty of Science and Technology, Phetchaburi Rajabhat University, Phetchaburi 76000, THAILAND

[2]Huahin Vitthayalai School, Hua–Hin, Prachuap Khiri Khan 77110, THAILAND

[3]Education Program in Physics, Faculty of Education, Silpakorn University, Nakhon Pathom 73000, THAILAND

[4]The demonstration school of Silpakorn University, Nakhon Pathom 73000, THAILAND

[5]Faculty of Engineering, Thonburi University, Bangkok 10160, THAILAND

[*]Corresponding author e-mail: sunantasak.rav@mail.pbru.ac.th

ARTICLE INFO

Article history:
Received: 6 November, 2020
Revised: 8 January, 2021
Accepted: 18 January, 2021
Available online: 27 September, 2021
DOI: 10.14456/jarst.2021.5

Keywords: buildup factors, fast neutron, plastic, polymer

ABSTRACT

This work discussed the theory of radiation shielding for some plastics and polymers. There were 6 samples for this study. They were bone-equivalent plastic (B-100), polyvinyl chloride (PVC), air equivalent plastic (C-552), radio chromic dye film (nylon base), polyethylene terephthalate (mylar) and polymethyl methacrylate (PMMA). These samples were simulated in term of photon and neutron shielding behaviors. Consequently, the theoretical study were separated into 2 types for photon shielding and neutron shielding. The geometrical progression (G-P) method was used to stimulate energy absorption build-up factor (EABF) and exposure build-up factor (EBF), at photon energies ranging from 15 keV to 15 MeV and up to 40 deep penetration mean free path (mfp) for photon shielding. Moreover, fast neutron removal cross-section (Σ_R) values were estimated by partial density method. The data of the simulation were found that equivalent atomic number (Z_{eq}) polymethyl methacrylate (PMMA) had the lowest values whereas EABF and EBF values had maximum values. Furthermore,

Journal of Applied Research on Science and Technology (JARST), Vol 20, Issue 2, 2021
ISSN: 2773-9376 (Print), 2773-9473 (Online)

polyvinyl chloride (PVC) had the highest equivalent atomic number (Z_{eq}) values whereas EABF and EBF values had the lowest values. The result for main interaction of photon with matter can be separated on energy regions that is photoelectric absorption (PE), Compton scattering (C) and pair production (PP) interactions. PE is main interaction at low energies ranging, C is main interaction at intermediate energies ranging and PP is main process at high energies ranging. The results indicated that polyvinyl chloride (PVC) exhibited excellent radiation shielding. Other than fast neutron removal cross-section value (Σ_R) of plastics and polymers, which estimated by partial density method, it was found that radio chromic dye film (nylon base) had the highest value. This result indicated that radio chromic dye film (nylon base) was the excellent neutron shielding material.

INTRODUCTION

Today, there are use of isotope in different sectors such as nuclear reactors, agriculture and medicine. The radiations from isotope are very dangerous not only harmful for man but include animal and environment. In the field of radiation physics, X/γ rays and neutrons are important subject for the study on radiation shielding (1,2). Build-up factors (BFs) and fast neutron removal cross section (Σ_R) are fundamental quantity to explain shielding of X/γ rays and neutrons, respectively. Materials used to against radiation should have high atomic number (high Z) while low atomic number (low Z) required for neutron (3).

There are many methods for simulating build-up factors like Geometrical Progression (G-P) fitting method. The American Nuclear Society used codes for computing photon energies ranging 15 keV-15 MeV up to deep penetration 40 mfp for 23 elements, one compound; water, and two mixture; air and concrete (4). Many researchers used G-P fitting method to study radiation shielding properties and reported that many materials such as inorganic scintillator, glasses, and alloy (5-7).

Plastics and polymers are long arrangement molecules and basic material used for against neutron and radiation because of low cost, low weight, friendly for environment, corrosion resistance, effective against radiation and high-Z nano- and micro-materials dispersed in polymer matrices have shown the enhancement ability in attenuating and absorbing high energy radiation (4,8-11,18). So, the authors interest to study the radiation shielding and Σ_R properties for some plastics and polymers. Radiation shielding properties were estimated and build-up factors by G-P fitting method and Σ_R properties were estimated by partial density method.

Table 1 Composition of plastics and polymers (2).

sample	code	%wt of each element							
		H	C	N	O	F	Ca	Cl	Si
Bone-equivalent plastic (B-100)	P1	0.0655	0.5370	0.0216	0.0321	0.1675	0.1766	-	-
Polyvinyl Chloride (PVC)	P2	0.0484	0.3844	-	-	-	-	0.5673	-
Air equivalent plastic (C-552)	P3	0.0247	0.5017	-	0.0046	0.4653	-	-	0.0040
Radio chromic dye film (nylon base)	P4	0.1020	0.6244	0.0989	0.1447	-	-	-	-
Polyethylene terephthalate (mylar)	P5	0.0420	0.6251	-	0.3331	-	-	-	-
Polymethyl methacrylate (PMMA)	P6	0.0806	0.5999	-	0.3197	-	-	-	-

MATERIALS AND METHODS

The chemical compositions of samples are exhibited in Table 1.

Build–up factors (BFs)

The determination of attenuation coefficient for γ–ray was made by investigating the transmitted radiation intensity I that pass through thickness x as compared to incident radiation intensity I_0. The linear attenuation coefficient (μ) was explained from exponential Beer–Lambert's law (19):

$$I = I_0 \cdot e^{-\mu x} \quad (1)$$

The build–up factors (BFs) are basically value used to design medium for radiation shielding. BFs are separated into two types, 1. energy absorption build-up factor (EABF) and 2. exposure build-up factor (EBF) which obtained by computing from Geometrical Progression (G-P) fitting method at energies ranging 0.015-15 MeV and these values are defined by Eq. (3-4). Firstly, it is very important to know about equivalent atomic number (Z_{eq}) values as this value must lie at specific energy between Z_1 and Z_2 atomic numbers ($Z_1 < Z_{eq} < Z_2$) which obtained by Eq. (2): (12-15).

$$Z_{eq} = \frac{Z_1(\log R_2 - \log R) + Z_2(\log R - \log R_1)}{\log R_2 - \log R_1} \quad (2)$$

where Z_1 and Z_2 are values of atomic numbers of elements according to ratios R_1 and R_2, respectively. R is ratio $(\mu_m)_{Compton}/(\mu_m)_{Total}$ for sample at same energy.

$$B(E, x) = 1 + (b-1)\{(K^x-1)/(K-1)\}, K \neq 1 \quad (3)$$

$$B(E, x) = 1 + (b-1)\,x, K = 1 \quad (4)$$

here K (E, x), photon dose multiplication factor, b, build-up factor corresponding to 1 mfp which obtained by Eq. (5):

ISSN: 2773-9376 (Print), 2773-9473 (Online)

$$K(E,x)=cx^{a}+d\frac{\tanh\left(\frac{x}{x_k}-2\right)-\tanh(-2)}{1-\tanh(-2)}, \quad (5)$$

$x \leq 40 \text{mfp}$

Lastly, fast neutrons removal cross sections (Σ_R) for samples can be computed using Eq. (6, 7) (16,17):

$$\sum_{R/\rho}=\sum_i w_i\left(\sum_{R/\rho}\right)_i \quad (6)$$

$$\sum_R=\sum_i \rho_i\left(\sum_{R/\rho}\right)_i \quad (7)$$

where $(\Sigma_{R/\rho})_i$ and ρ_i are mass removal cross section and partial density of i^{th} element, respectively.

RESULT AND DISCUSSION

Z_{eq} of plastics and polymers for photon energy 15 keV-15 MeV are shown in Figure 1. The energy, deep penetration and samples dependency of EABF and EBF values are exhibited in Figures 2-5, respectively. The effective of Σ_R is shown graphically in Figure 6.

EABF and EBF with energy

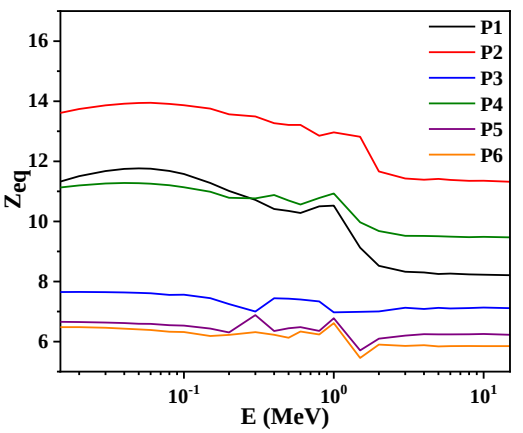

Figure 1 Z_{eq} of samples at energies ranging of 15 keV-15 MeV.

Figure 1 shows Z_{eq} for samples with energies in the range 15 keV to 15 MeV and up to 40 deep penetration mean free path (mfp). It was found that polyvinyl chloride (PVC), P2, possesses highest Z_{eq} values. The graphs were not smooth because of K- edge absorption of Ca (4.04×10^{-3} MeV), Cl (2.82×10^{-3} MeV) and Si (1.84×10^{-3} MeV) and content of composition elements in samples as shown in Table 1.

The EABF and EBF for plastics and polymers samples with energies at fixed deep penetration are shown in Figure 2 and 3. From the figures, it can be separated into three energy regions: photoelectric absorption (PE), Compton scattering (C) and pair production (PP), respectively, as main interactions (3). PE is main interaction at low energies ranging, and BFs of samples have small value in this energy ranging. While C is main interaction at intermediate energies ranging, EABF and EBF values increase rapidly with increasing photon energies for all samples. After that, EABF and EBF values decrease which PP is main process at high energies ranging. This figure presents that EABF and EBF maximum value were dependent on deep penetration and composition of plastics and polymers materials. EABF and EBF values increase until they reach maximum value and then decrease with increasing energies. That can be discussed on fundamental of partial interaction processes. At low energies ranging, EABF and EBF values are lowest because of photons were absorbed at high energy. At intermediate ranging, EBF and EABF values were largest because of photons were degradant by scattering in medium. The highest EABF and EBF values were observed at 40 mfp, deep penetration while the lowest values were shown at 1 mfp. At high energy ranging, photons were absorbed again. The sharp peak of EABF and EBF at high energy and deep penetration were occurred because of electron-positron annihilation in material and then produced

secondary photons. In really, increasing of deep penetration for medium leading to increase thickness of interacting medium as according to high equivalent atomic number as shown in Figure 1. The graphs were not continuous because of K- edge absorption of Ca (4.04×10^{-3} MeV), Cl (2.82×10^{-3} MeV) and Si (1.84×10^{-3} MeV).

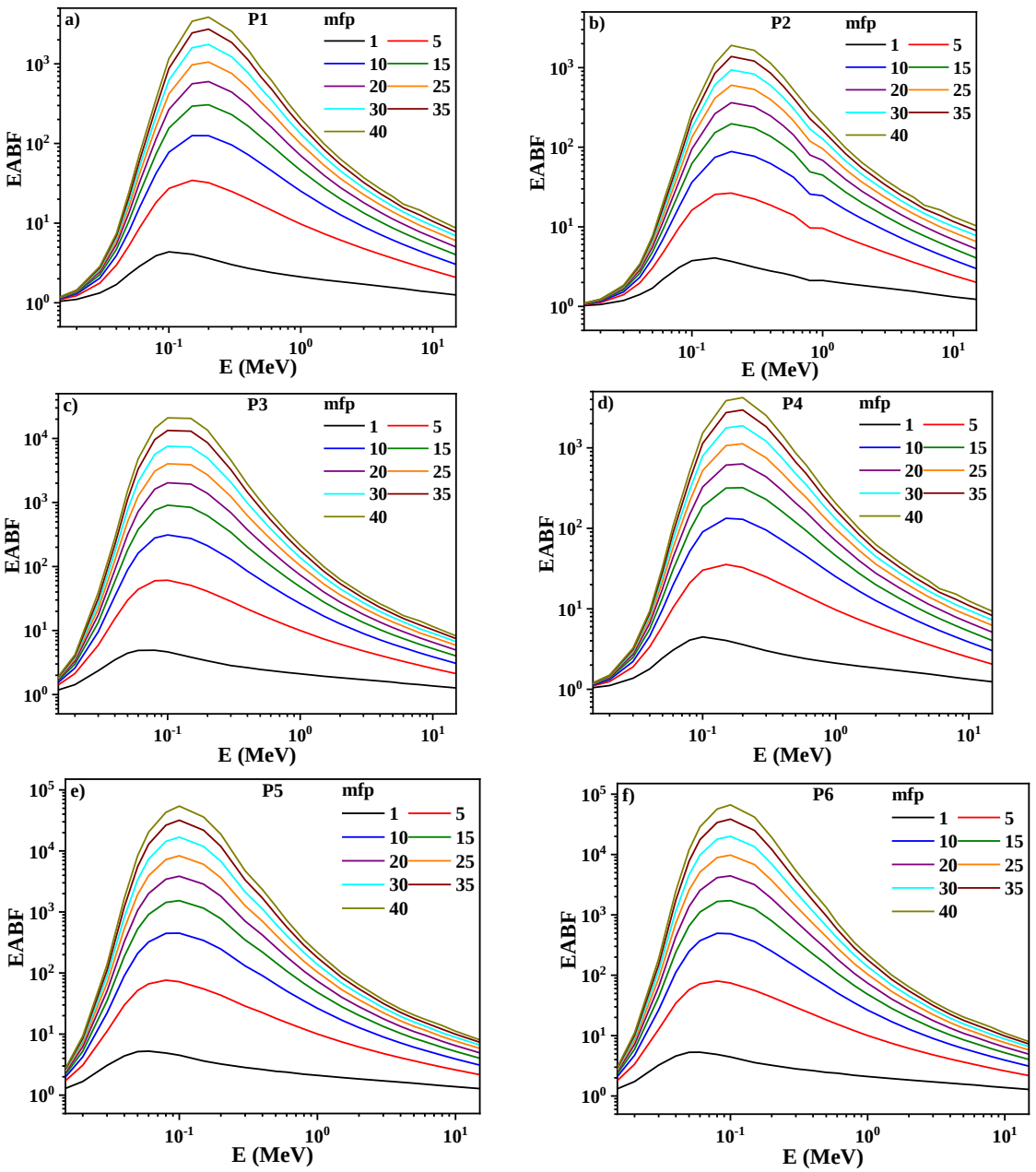

Figure 2 (a-f). EABF at energies ranging 0.015–15 MeV up to 40 mfp for samples.

Journal of Applied Research on Science and Technology (JARST), Vol 20, Issue 2, 2021
ISSN: 2773-9376 (Print), 2773-9473 (Online)

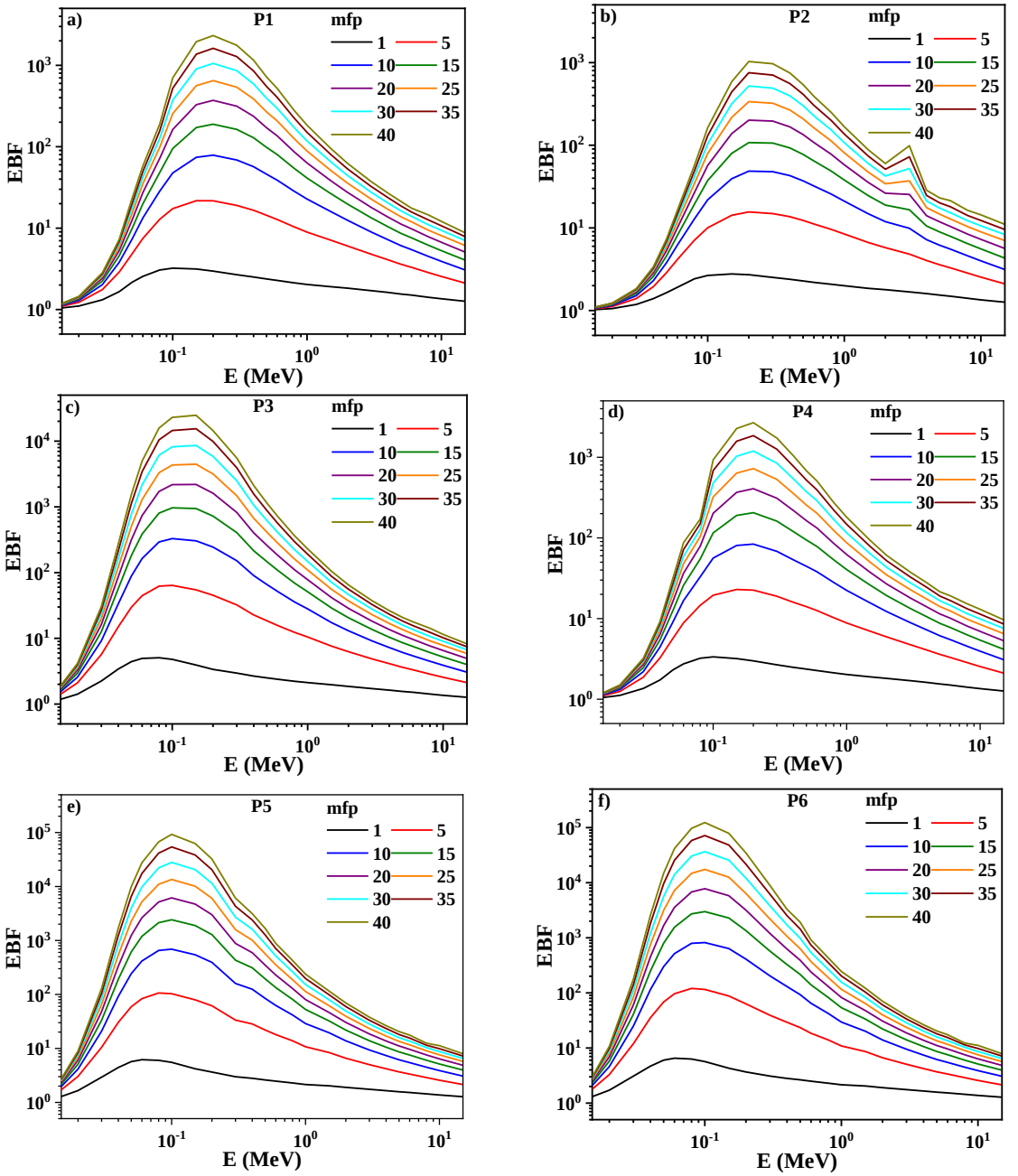

Figure 3 (a-f). EBF at energies ranging 0.015–15 MeV up to 40 mfp for samples.

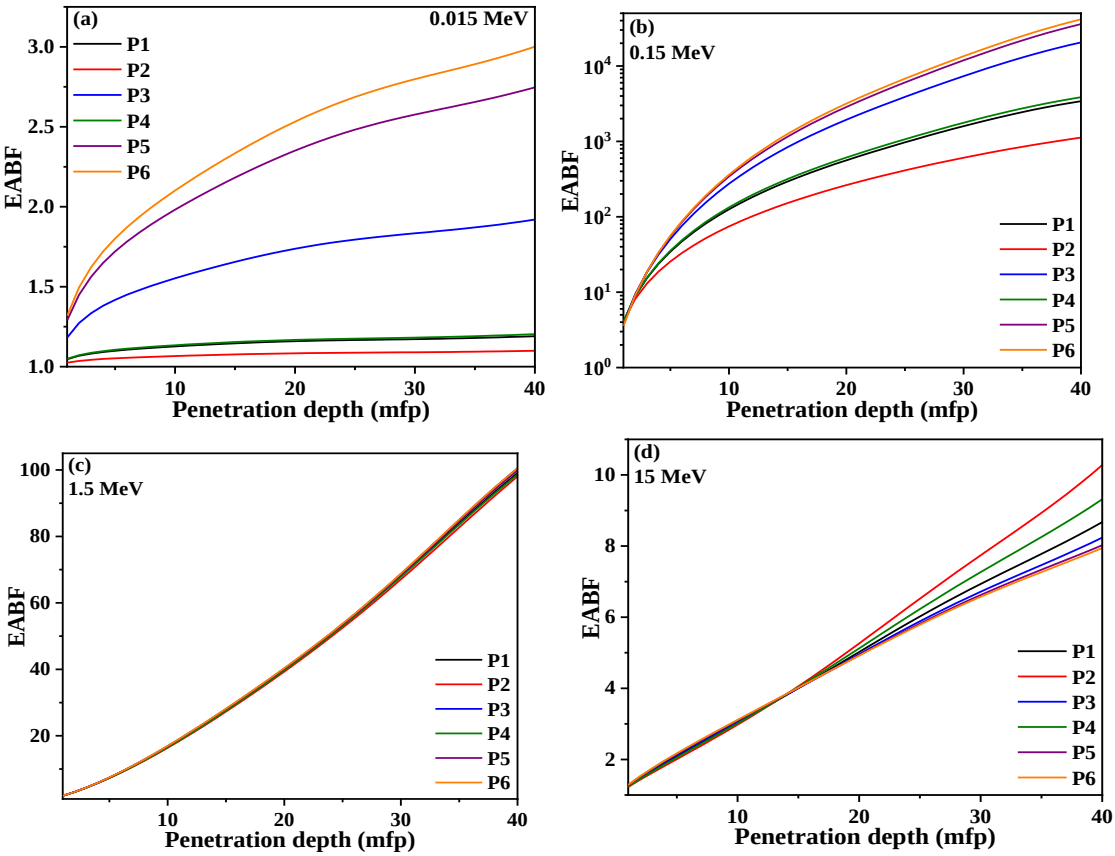

Figure 4 (a-d). EABF of samples at 0.015, 0.15, 1.5, 15 MeV up to 40 mfp.

EABF and EBF with deep penetration

EABF and EBF values of samples with deep penetration are shown in Figures 4 and 5 (a–d), respectively, at energies (0.015, 0.15, 1.5 and 15 MeV). From these figures, EABF and EBF values increase with increasing deep penetration. At 0.015, 0.15 and 1.5 MeV, EABF and EBF values of all samples varies directly with Z_{eq} and the lowest values of EABF and EBF are P2 sample. At energy 15 MeV, P6 showed highest EABF and EBF values that because of pair/triplet interaction of samples produced electron/positron pair. The rest of positrons were annihilated by electron and generate two secondary photons at energy 0.511 MeV. Photons probability for escape through higher thickness of samples were increased, resulting in larger EABF and EBF values. Finally, the excellent radiation shielding medium, low values of buildup factors were desired.

Fast neutron removal cross-section (Σ_R)

The fast neutron removal cross-section Σ_R (cm^{-1}) value of plastics and polymers are exhibited in Figure 6. It was found that Σ_R (cm^{-1}) of radio chromic dye film (nylon base), P4, was highest. Therefore, P4 is the best neutron shielding compared with other samples.

Journal of Applied Research on Science and Technology (JARST), Vol 20, Issue 2, 2021
ISSN: 2773-9376 (Print), 2773-9473 (Online)

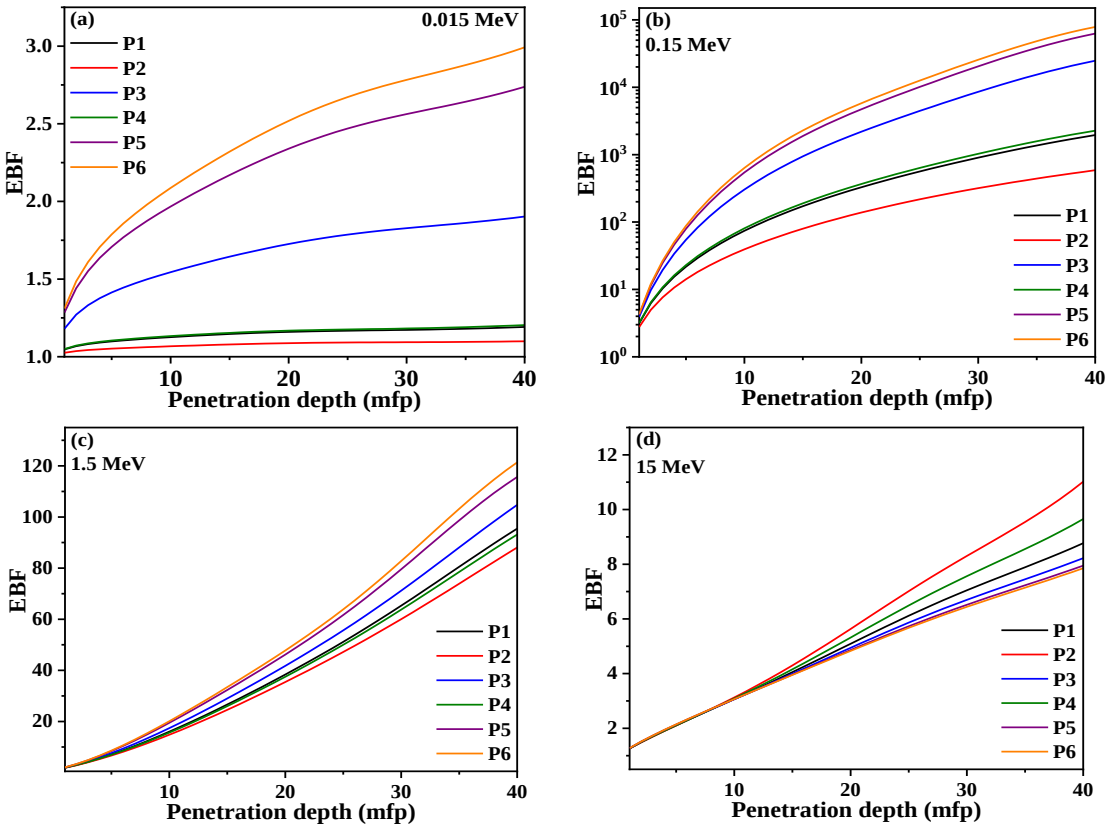

Figure 5 (a-d). EBF for samples at 0.015, 0.15, 1.5, 15 MeV up to 40 mfp.

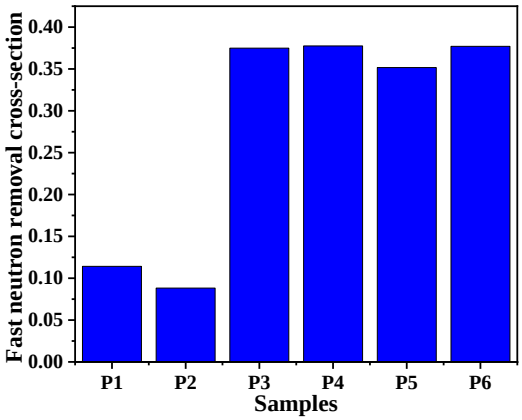

Figure 6 The effective removal cross sections for fast neutrons (Σ_R) for all samples.

CONCLUSION

From the present study, EABF and EBF values of plastic and polymer samples are maximum values at intermediate energies ranging, where Compton scattering is main interaction. Z_{eq} for polymethyl methacrylate (PMMA: P6) has lowest values whereas EABF and EBF values have maximum, while polyvinyl chloride (PVC: P2) has highest Z_{eq} values whereas lowest for EABF and EBF values. The results exhibited that polyvinyl chloride (PVC: P2) has more shielding effectiveness

for radiation material. Finally, for neutron shielding, polymethyl methacrylate (PMMA: P6) has more shielding effectiveness.

ACKNOWLEDGEMENT

In this study, the authors would like to thank Phetchaburi Rajabhat University for its support instrument.

REFERRENCES

1. Vishwanath PS, Badiger NM, Chanthima N, Kaewkhao J. Evaluation of gamma-ray exposure buildup factors and neutron shielding for bismuth borosilicate glasses. Radiat Phys Chem. 2014;98:14-21.
2. Gurler O, Tarim UA. Determination of Radiation Shielding Properties of Some Polymer and Plastic Materials against Gamma-Rays. Acta Phys Pol A. 2016;130:236-8.
3. Agar O, Kavaz E, Altunsoy EE, Kilicoglu O, Tekin HO, Sayyed MI, et al. Er_2O_3 effects on photon and neutron shielding properties of TeO_2-Li_2O-ZnO-Nb_2O_5 glass system. Results Phys. 2019;13:102277.
4. Kaur P, Devinder S, Tejbir S. Gamma rays shielding and sensing application of some rare earth doped lead-alumino-phosphate glasses. Radiat Phys Chem. 2018;144:336-43.
5. Issa SAM, Sayyed MI, Zaid MHM, Matori KA. A comprehensive study on gamma rays and fast neutron sensing properties of GAGOC and CMO scintillators for shielding radiation applications. J Spectrosc. 2017;9792816:1-9.
6. Tekin HO, Altunsoy EE, Kavaz E, Sayyed MI, Agar O, Kamislioglu M. Photon and neutron shielding performance of boron phosphate glasses for diagnostic radiology facilities. Results Phys. 2019;12:1457-64
7. Vishwanath PS, Badiger NM. Gamma ray and neutron shielding properties of some alloy materials. Ann Nucl Energy. 2014;64:301-10.
8. Kadhim LF. Mechanical properties of high-density polyethylene/chromium trioxide under ultraviolet rays. International Journal of Applied Engineering Research. 2017;12(10):2517-26.
9. Mahmoud ME, El-Sharkawy RM, Allam EA, Elsaman R, El-Taher A. Fabrication and characterization of phosphotungstic acid - Copper oxide nanoparticles - Plastic waste nanocomposites for enhanced radiation-shielding. J Alloy Compd. 2019;803:768-77.
10. Mahmoud KA, Lacomme E, Sayyed MI, Ozpolat OF, Tashlykov OL. Investigation of the gamma ray shielding properties for polyvinyl chloride reinforced with chalcocite and hematite minerals. Heliyon. 2020;6:e03560.
11. Labouriau A, Robison T, Shonrock C, Simmonds S, Cox B, Pacheco A, et al. Boron filled siloxane polymers for radiation shielding. Radiat Phys Chem. 2018;144:288-94.
12. Sayyed MI, AlZaatreh MY, Matori KA, Sidek HAA, Zaid MHM. Comprehensive study on estimation of gamma-ray exposure buildup factors for smart polymers as a potent application in nuclear industries. Results Phys. 2018;9:585-92.
13. Şakar E. Determination of photon-shielding features and build-up factors of nickel–silver alloys. Radiat Phys Chem. 2020;172:108778.
14. Tekin HO, Kilicoglu O, Kavaz E, Altunsoy EE, Almatari M, Agar O, et al. The investigation of gamma-ray and neutron shielding parameters of Na_2O-CaO-P_2O_5-SiO_2 bioactive glasses using MCNPX code. Results Phys. 2019;12:1797-804.

ISSN: 2773-9376 (Print), 2773-9473 (Online)

15. Sayyed MI, Elhouichet H. Variation of energy absorption and exposure buildup factors with incident photon energy and penetration depth for boro-tellurite (B_2O_3-TeO_2) glasses. Radiat Phys Chem. 2017;130:335-42

16. Dong MG, Sayyed MI, Lakshminarayana G, Ersundud MÇ, Ersundu AE, Nayare P, et al. Investigation of gamma radiation shielding properties of lithium zinc bismuth borate glasses using XCOM program and MCNP5 code. J Non-Cryst Solids. 2017;468:12-6.

17. Oto B, Yıldız N, Korkutb T, Kavazc E. Neutron shielding qualities and gamma ray buildup factors of concretes containing limonite ore. Nucl Eng Des. 2015;293:166-75

18. Da C, Ge Y, Mohamed B, Dan M. Gamma radiation shielding properties of poly (methyl methacrylate) /Bi_2O_3 composites. Nucl Eng Technol. 2020;52: 2613-19.

19. Ahmed SO. Development of high–performance heavy density concrete using different aggregates for gamma-ray shielding. Prog Nucl Energ. 2015;79:48–55.